Ann Thorac Surg
2009;87:906–10



*Table 3. Characteristics of Patients With Identifiable and Nonidentifiable Sentinel Lymph Nodes With Tin Colloid*

| Variable | Sentinel Lymph Nodes | | |
|---|---|---|---|
| | Identifiable | Nonidentifiable | Difference |
| Age (y) | | | |
| Mean ± SD | 69 ± 7 | 72 ± 7 | NS |
| Range | 53–81 | 59–82 | |
| Tumor size (cm) | | | |
| Mean ± SD | 2.0 ± 0.8 | 2.2 ± 0.8 | NS |
| Range | 0.8–4.0 | 1.1–4.5 | |
| Operative procedure | | | |
| Lobectomy/ segmentectomy | 14/40 | 5/14 | NS |
| $FEV_1$/FVC (%) | | | |
| Mean ± SD | 72 ± 10 | 66 ± 10 | $p = 0.04$ |
| Range | 44–87 | 47–91 | |
| Pathologic N stage | | | NS |
| N0 | 49 | 18 | |
| N1 | 3 | 0 | |
| N2 | 2 | 1 | |
| Total | 54 | 19 | |

$FEV_1$ = forced expiratory volume in 1 second; FVC = forced vital capacity; NS = not significant; SD = standard deviation.

### *Statistical Analysis*

Differences in identification rate, sex, operative procedure, and pathologic N stage between the tin colloid and phytate groups were analyzed for statistical significance using the $\chi^2$ test. Differences in the number of SNs, the radioactivity count of SNs, and age between the groups were analyzed for statistical significance using the Student's *t* test. Probability values of less than 0.05 were accepted as indicating statistical significance. All values in the text and tables are given as mean ± standard deviation.

*Table 4. Patient Characteristics With Identifiable and Nonidentifiable Sentinel Lymph Nodes With Phytate*

| Variable | Sentinel Lymph Nodes | | |
|---|---|---|---|
| | Identifiable | Nonidentifiable | Difference |
| Age (y) | | | |
| Mean ± SD | 63 ± 10 | 64 ± 8 | NS |
| Range | 36–81 | 48–74 | |
| Tumor size (cm) | | | |
| Mean ± SD | 1.8 ± 0.8 | 1.6 ± 0.6 | NS |
| Range | 0.7–5.0 | 0.6–2.8 | |
| Operative procedure | | | |
| Lobectomy/ segmentectomy | 14/52 | 4/4 | NS |
| $FEV_1$/FVC (%) | | | |
| Mean ± SD | 74 ± 9 | 74 ± 7 | NS |
| Range | 37–91 | 60–84 | |
| Pathologic N stage | | | NS |
| N0 | 60 | 7 | |
| N1 | 1 | 0 | |
| N2 | 5 | 1 | |
| Total | 66 | 8 | |

$FEV_1$ = forced expiratory volume in 1 second; FVC = forced vital capacity; NS = not significant; SD = standard deviation.

*Table 5. Sentinel Node Mapping by Tin Colloid and Phytate*

| Station | Number of Patients (%) | | |
|---|---|---|---|
| | Tin Colloid | Phytate | Difference |
| Hilum (total)[a] | 50/54 (93) | 58/66 (88) | NS |
| Hilar | 9/54 (17)[b] | 19/66 (28)[c] | NS |
| Interlobar | 8/54 (15)[b] | 20/66 (30)[d] | NS |
| Lobar | 24/54 (44) | 27/66 (41) | NS |
| Segmental | 28/54 (52) | 34/66 (52) | NS |
| Mediastinum (total) | 19/54 (35) | 39/66 (59) | $p = 0.01$ |
| Upper mediastinum | 14/54 (26) | 29/66 (44) | NS |
| Lower mediastinum | 7/54 (13) | 18/66 (27) | NS |

[a] Sentinel nodes were identified less frequently in the hilar and interlobar stations than in the segmental station. [b] $p < 0.001$ vs segmental station. [c] $p = 0.01$ vs segmental station. [d] $p = 0.02$ vs segmental station.

NS = not significant.

## Results

Table 2 shows the results of SN identification in the tin colloid and phytate groups. The SNs were identifiable in 54 of 73 patients (74%) in the tin colloid group, which was significantly lower than the 89% (66 of 74 patients) identified in the phytate group ($p = 0.02$). The mean number of SNs identified by tin colloid was 1.7 ± 0.8 nodes/patient, which was significantly less than the 2.4 ± 1.5 in the phytate group ($p = 0.002$). The mean radioactivity of the hottest SNs counted by the gamma probe were 121 ± 186 and 208 ± 880 in the tin colloid and phytate groups, respectively, of which the difference was not significant.

Table 3 shows the characteristics of patients with identifiable and nonidentifiable SNs in the tin colloid group. The mean $FEV_1$/FVC in 19 patients with nonidentifiable SNs was 66% ± 10%, which was significantly lower than the 72% ± 10% in 54 patients with identifiable SNs ($p = 0.04$). There were no significant differences in age, tumor size, operative procedure, or pathologic N stage between patients with and without identifiable SNs.

Table 4 shows the characteristics of patients with identifiable and nonidentifiable SNs in the phytate group. There were no significant differences in these factors, including $FEV_1$/FVC, between patients with and without identifiable SNs.

Table 5 shows the SNs identified at the hilum and mediastinum in the tin colloid and phytate groups. In both groups, segmental stations were more frequently identified as SNs than hilar or interlobar stations ($p = 0.02$ to $p < 0.001$). Whereas the SN identification rate did not differ significantly between the two groups at the

*Table 6. Sentinel Node Identification in Patients With N1 or N2 Disease*

| No. | Age/Sex | Tumor Location | *p*-TNM | Sentinel Node | Lymph Node With Metastasis |
|---|---|---|---|---|---|
| Tin colloid | | | | | |
| 1 | 70/M | RLL | T1N1M0 | #13 | #13 |
| 2 | 54/F | LLL | T1N2M0 | #12 | #7, 11, 12 |
| 3 | 72/M | RLL | T1N1M0 | #11 | #11 |
| 4 | 80/M | LUL | T1N2M0 | #5 | #5, 12, 13 |
| 5 | 75/M | LLL | T1N1M1 | #10, 13 | #13 |
| 6 | 69/M | RML | T1N2M0 | not identified | #1, 2, 3, 4, 11, 12 |
| Phytate | | | | | |
| 1 | 70/F | RUL | T1N1M0 | #4, 7, 12, 13 | #13 |
| 2 | 81/M | LUL | T1N2M0 | #4, 5 | #5 |
| 3 | 44/F | RML | T1N2M0 | #7, 10 | #7 |
| 4 | 68/M | LUL | T2N2M0 | #5, 7, 11, 13 | #5 |
| 5 | 61/F | RLL | T2N2M0 | #7, 12 | #7, 11, 12 |
| 6 | 50/F | LUL | T1N2M0 | #5 | #5, 10 |
| 7 | 69/F | LUL | T4N2M0 | not identified | #5, 7, 10, 11, 12, 13 |

LLL = left lower lobe; LUL = left upper lobe; RLL = right lower lobe; RML = right middle lobe; RUL = right upper lobe.



hilum, tin colloid identified SNs at the mediastinum in 19 of the 54 patients (35%), which was significantly lower than the 58% (39 of the 66 patients) identified in the phytate group ($p = 0.01$).

Six and 7 patients had pathologic N1 or N2 disease in the tin colloid and phytate groups, respectively (Table 6). Sentinel nodes could not be identified in 1 patient each of the two groups, because their hilar and mediastinal lymph nodes were completely occupied by metastatic tumors, which could be seen macroscopically during surgery. The remaining 5 and 6 patients with N1 or N2 disease in the tin colloid and phytate groups, respectively, had identifiable SNs. All of these 11 patients had metastases in SNs, resulting in the false-negative rate for SN identification being 0% in both groups. Even in 3 patients with skip metastasis to mediastinal lymph nodes (patients 2, 3, and 4 in the phytate group), the SN identification procedure detected these skip metastases. All 5 patients with N1 or N2 disease in the tin colloid group had metastases in the SNs with the highest radioactivity. On the other hand, of the 6 patients with N1 or N2 disease in the phytate group, 4 had metastases in the SNs with the highest radioactivity, whereas the remaining 2 patients had metastases in the SNs with the second or fourth highest radioactivity but not in that with the highest radioactivity.

## Comment

The present study showed both the tin colloid and phytate to be capable of detecting metastatic SNs in patients with clinical stage I NSCLC. Our previous studies demonstrated the following advantages of identifying the SN in patients with NSCLS: (1) measurement of radioactivity in mediastinal lymph nodes before dissection, ie, in vivo identification of SN, could identify mediastinal SN, which allows mediastinal lymph node dissection to be minimized [7]; and (2) intraoperative N staging by submitting SNs for frozen section can determine the final indication for segmentectomy [8]. The results of the present study and our previous report allow us to conclude that SN identifications, using both tin colloid and phytate, can minimize the mediastinal lymph node dissection and determine the final indication of segmentectomy in patients with clinical stage I NSCLC.

Although there have been no reports comparing the identification rate of SNs between tin colloid and phytate in patients with NSCLC, several reports on breast cancer have compared the rates between these two tracers, showing the identification rate with tin colloid to range from 36% to 63%, ie, generally lower than the 82% to 100% range with phytate [2, 12, 13]. Higashi and colleagues [14] examined the particle size of tin colloid at various ratios of a mixture of isotonic sodium chloride and tin colloid solution, showing mean particle sizes of 47, 96, 712, 925, and 1,079 nm at the ratios of 1:4, 1:2, 1:1, 2:1, and 4:1, respectively. In the present study, the ratio of $^{99m}$Tc and tin colloid was adjusted to 1:1 to make the $^{99m}$Tc-tin colloid in a volume of 1 to 1.5 mL have a radioactivity of 6 to 8 mCi. Therefore, based on the data of Higashi and coworkers [14], the particle size of tin colloid in our present study would be approximately 712 nm, ie, larger than that of phytate at 200 to 400 nm [2, 3]. We demonstrated herein that phytate, owing to its smaller particle size, more frequently identifies SNs in patients with NSCLC than tin colloid.

The present results show the $FEV_1$/FVC ratio to be significantly lower in patients with nonidentifiable SNs than in those with identifiable SNs in the tin colloid group, results consistent with those of our previous study [6]. On the other hand, the phytate group showed no difference in $FEV_1$/FVC between patients with and without identifiable SNs. In breast cancer, the SN identification rate is reported to be lower in older than in younger

patients, which is attributable to breast tissue gradually being replaced by fat and decreased lymphatic vessel density with aging [15]. We consider that the lung tissue in patients with chronic obstructive pulmonary disease could also possibly have a lower density of lymphatic vessels or lower lymphatic flow than normal lung tissue, a situation comparable to that in breast tissue, which may account for the lower SN identification rate with the tin colloid tracer. However, the phytate might flow through lymphatic vessels more easily and thereby arrive at SNs even in chronic obstructive pulmonary disease patients because of its smaller particle size as compared with tin colloid. We therefore consider phytate to be more appropriate than tin colloid for patients with chronic obstructive pulmonary disease.

The present study showed that although the number of SNs identified by tin colloid was higher than that by phytate, the lower number of SNs identified by the former was not associated with false-negative results in patients with N1 or N2 disease. Therefore, tin colloid can detect metastatic lymph nodes with fewer number of SNs submitted for intraoperative frozen section, as compared with phytate. In addition, the SNs with the highest radioactivity identified by tin colloid were consistently metastatic lymph nodes. This is probably attributable to the tin colloid being retained within a true SN for a relatively long time because of its large particle size. On the other hand, the SNs with the highest radioactivity identified by phytate were not always metastatic lymph nodes, probably because phytate can pass through the true SN relatively easily and continue to flow further up the chain of nodes because of its small particle size.

We conclude that phytate more frequently identifies SNs than tin colloid, even in patients with low $FEV_1/FVC$ ratios, whereas the latter can identify SNs with fewer number of lymph nodes examined, thereby allowing the number of SNs submitted for intraoperative frozen section examination to be reduced. Although we are now using phytate for SN identification in patients with clinical stage Ia NSCLC, the limitation of this tracer should be kept in mind, ie, the SNs showing the highest radioactivity identified by phytate are not always metastatic lymph nodes.

This work was supported, in part, by a Grant-in-Aid from the Ministry of Health, Labor and Welfare of Japan.

## References

1. Shimazu K, Tamaki Y, Taguchi T, Takamura Y, Nobuchi S. Comparison between periareolar and peritumoral injection of radiotracer for sentinel lymph node biopsy in patients with breast cancer. Surgery 2002;131:277–86.
2. Tsugawa K, Inokuchi M, Miwa K, Noguchi M. Sentinel lymph node biopsy of breast cancer using blue dye and radioisotope. J Jpn Surg Soc 2001;102(Suppl):373 (in Japanese).
3. Campbell J, Bellen JC, Baker RJ, Cook DJ. Technetium-99m calcium phytate–optimization of calcium content for liver and spleen scintigraphy: concise communication. J Nucl Med 1981;22:157–60.
4. Liptay MJ, Masters GA, Winchester DJ, et al. Intraoperative radioisotope sentinel lymph node mapping in non-small cell lung cancer. Ann Thorac Surg 2000;70:384–90.
5. McMasters KM, Reintgen DS, Ross MI, et al. Sentinel lymph node biopsy for melanoma: how many radioactive nodes should be removed? Ann Surg Oncol 2001;8:192–7.
6. Nomori H, Horio H, Naruke T, Orikasa H, Yamazaki K, Suemasu K. Use of technetium-99m tin colloid for sentinel lymph node identification in non-small cell lung cancer. J Thorac Cardiovasc Surg 2002;124:486–92.
7. Nomori H, Watanabe K, Ohtsuka T, Naruke T, Suemasu K. In vivo identification of sentinel nodes for clinical stage I non-small cell lung cancer for abbreviation of mediastinal lymph node dissection. Lung Cancer 2004;46:49–55.
8. Nomori H, Ikeda K, Mori T, et al. Sentinel node navigation segmentectomy for c-T1N0M0 non-small cell lung cancer. J Thorac Cardiovasc Surg 2007;133:780–5.
9. Nomori H, Ikeda K, Mori T, Shiraishi S, et al. Sentinel node identification in clinical stage Ia non-small cell lung cancer by a combined single photon emission computed tomography/computed tomography system. J Thorac Cardiovasc Surg 2007;134:182–7.
10. Naruke T, Suemasu K, Ishikawa S. Lymph node mapping and curability at various levels of metastasis in resected lung cancer. J Thorac Cardiovasc Surg 1978;76:832–9.
11. Nomori H, Horio H, Naruke T, Suemasu K. What is the advantage of a thoracoscopic lobectomy over a limited thoracotomy procedure for lung cancer surgery? Ann Thorac Surg 2001;72:879–84.
12. Shimizu Y, Miyauchi M, Yamamoto N, et al. Sentinel node navigation surgery (tin colloid versus stannous phytate). Proceedings of the 9th Annual Meeting of the Japanese Breast Cancer Society, Maebashi, Japan, July, 2001, *p* 124 (in Japanese).
13. Suzuki K, Kobayashi Y, Miyata K, et al. Experience of 99m-Tc stannous phytate in the identification of sentinel lymph nodes. Proceedings of the 9th Annual Meeting of the Japanese Breast Cancer Society, Maebashi, Japan, July, 2001, *p* 124 (in Japanese).
14. Higashi H, Matsugoe S, Uenosono Y, et al. Particle size of tin and phytate colloid in sentinel node identification. J Surg Res 2004;121:1–4.
15. Tefra L, Lannin DR, Swanson MS, et al. Multicenter trial of sentinel node biopsy for breast cancer using both technetium sulfur colloid and isosulfan blue dye. Ann Surg 2001; 233:51–9.

ELSEVIER

European Journal of Cardio-thoracic Surgery 35 (2009) 408–413

EUROPEAN JOURNAL OF CARDIO-THORACIC SURGERY

www.elsevier.com/locate/ejcts

# Prediction of pulmonary function after lung lobectomy by subsegments counting, computed tomography, single photon emission computed tomography and computed tomography: a comparative study

Kentaro Yoshimoto [a], Hiroaki Nomori [a,*], Takeshi Mori [a], Hironori Kobayashi [a], Yasuomi Ohba [a], Hidekatsu Shibata [a], Shinya Shiraishi [b], Toshiaki Kobayashi [c]

[a] Department of Thoracic Surgery, Graduate School of Medical Sciences, Kumamoto University, 1-1-1 Honjo, Kumamoto 860-8556, Japan
[b] Department of Diagnostic Radiology, Graduate School of Medical Sciences, Kumamoto University, 1-1-1 Honjo, Kumamoto 860-8556, Japan
[c] Department of Assistive Diagnostic Technology, National Cancer Center Hospital, 5-1-1 Tsukiji, Chuo-ku, 104-0045 Tokyo, Japan

Received 13 August 2008; received in revised form 20 October 2008; accepted 21 October 2008; Available online 21 January 2009

## Abstract

**Objective:** The aim of the present study was to determine the optimal method of predicting postoperative pulmonary function (PPF) after lung lobectomy. **Methods:** The forced expiratory volume in 1 s ($FEV_1$) was measured in 37 patients before and after lobectomy, and the following three methods of predicting the PPF were evaluated: (1) the number of functioning subsegments to be resected were counted (subsegments counting [SC]); (2) the volume of the functioning lung was calculated using CT images (quantitative CT); and (3) perfusion scintigraphy was performed using co-registered single photon emission computed tomography and CT imaging (SPECT/CT). The $FEV_1$ values predicted using these three methods were then compared with the measured postoperative $FEV_1$, and the correlations and differences were analyzed. **Results:** While a paired *t*-test showed the SPECT/CT method to have the smallest difference between the measured and the predicted $FEV_1$ values (0.05 l, $p = 0.33$), followed by the quantitative CT method (0.07 l, $p = 0.07$), and finally the SC method (0.15 l, $p < 0.001$), the difference between the two values was not significantly different between the quantitative CT and SPECT/CT method ($p = 0.22$). **Conclusions:** While the SC method is inferior to both the quantitative CT and the SPECT/CT methods for predicting the PPF after lobectomy, the latter two methods are almost equally accurate.


*Keywords:* Computed tomography; Single photon emission computed tomography; Pulmonary function; Surgery; Lung cancer

## 1. Introduction

Pulmonary function is an important factor for determining the indications for lung surgery. To predict the postoperative pulmonary function (PPF), calculating the number of lung subsegments to be resected is one of the simplest methods available, and this method has been reported to predict the PPF with an accuracy equal to that of scintigraphy [1–3]. A more detailed method consists of calculating the number of functioning subsegments to be resected, distinguishing between subsegments that are occluded and those that are unoccluded by the lesions [4]. However, in patients with chronic obstructive pulmonary disease (COPD) or interstitial pneumonia, these subsegment counting (SC) methods cannot predict PPF reliably, because emphysema and interstitial pneumonia are often not distributed uniformly.

While perfusion scintigraphy can be used to image the functioning lung, the SC method has been reported to predict PPF as accurately as perfusion scintigraphy [2–6]. However, the scintigraphy data in these reports were obtained from planar images, which cannot identify the boundaries between the lobes. Recent advances in single photon emission computed tomography (SPECT) have enabled images that are more precise than planar images to be obtained [7,8]. However, even in these new SPECT images, identifying the pulmonary lobes remains difficult, because the boundaries between the lobes are almost unrecognizable. To show the anatomy of the lung on SPECT images more accurately, a fused image of SPECT and multidetector CT images (SPECT/CT) has been used recently [9]; these images allow the boundaries between the lobes to be precisely identified.

On the other hand, the volume of the functioning lung can also be calculated from CT images with a CT number in the range of −910 to −500 Hounsfield Units (HU), i.e., the quantitative CT method. Because this range of CT numbers can be used to assess the extent of emphysema, this method

* Corresponding author. Tel.: +81 96 373 5533; fax: +81 96 373 5532.
*E-mail address:* hnomori@kumamoto-u.ac.jp (H. Nomori).

1010-7940/$ – see front matter 
doi:10.1016/j.ejcts.2008.10.057

is strongly correlated with pulmonary function [10–12]. Wu et al. reported that the quantitative CT method could predict the PPF as accurately as perfusion scintigraphy [13]. However, they compared the quantitative CT method with planar scintigraphic images, and not with SPECT or SPECT/CT.

In the present study, we evaluated the optimal method for predicting PPF in patients undergoing lobectomy by comparing the SC, quantitative CT and SPECT/CT methods.

## 2. Materials and methods

### 2.1. Eligibility

The study protocol for examining perfusion scintigraphy with SPECT/CT in patients undergoing major lung resection was approved by the ethics committee of Kumamoto University Hospital in April 2005. Informed consent was obtained from all patients after discussing the risks and benefits of the study.

### 2.2. Patients

Between June 2005 and October 2007, 79 patients underwent lobectomy for lung cancer in Kumamoto University Hospital. Of the 79 patients, 37 patients had SPECT/CT performed before surgery and the pulmonary function test before and after surgery (Table 1). The patients who underwent pneumonectomy were excluded in this study because planar image of perfusion scintigraphy is enough and SPECT/CT is not necessary for prediction of pulmonary function after pneumonectomy. None of the patients had underlying pulmonary diseases, such as interstitial lung disease, severe chronic obstructive lung disease, and infectious disease.

### 2.3. Pulmonary function test

Vital capacity (VC), forced vital capacity (FVC) and forced expiratory volume in 1 s ($FEV_1$) were measured with the patients in the seated position using a dry rolling-seal spirometer (CHESTAC-9800DN, CHEST Inc., Tokyo, Japan) in accordance with American Thoracic Society standards [14]. The preoperative pulmonary function test was conducted within one month prior to surgery, and the PPF was measured later than 6 months after the surgery (median: 6 months; range: 6–17 months).

Table 1
Patient characteristics.

| | |
|---|---|
| Male | 22 |
| Female | 15 |
| Mean age (y.o.) (range) | 65 ± 12 (30–80) |
| Site of lobectomy | |
| Right upper lobe | 5 |
| Right middle lobe | 4 |
| Right lower lobe | 7 |
| Left upper lobe | 7 |
| Left lower lobe | 8 |
| Right upper and middle lobes | 2 |
| Right middle and lower lobes | 4 |
| Mean preoperative FVC (l) | 3.22 ± 0.82 (5.06–1.88) |
| Mean preoperative $FEV_1$ (l) | 2.29 ± 0.59 (3.76–1.43) |
| Mean preoperative $FEV_1$/FVC (%) | 72.1 ± 10.5 (85.1–46.5) |

### 2.4. Subsegments counting

The PPF was predicted based on the number of functioning SC method using the following formula, according to the method by Nakahara et al. [4]:

Predictive postoperative $FEV_1 = [1 - (n - a)/(42 - a)] \times$ preoperative $FEV_1$, where $[n]$ is the total number of subsegments in the resected lobe, which is assumed to be 6, 4 and 12 for the right upper, middle and lower lobe, respectively, and 10 each for the left upper and lower lobes, and $[a]$ is the number of subsegments obstructed by tumors.

### 2.5. Quantitative CT

CT was performed at the end of full inspiration using 4 multidetector CT scanners (LightSpeed QX/i, GE Medical Systems, Milwaukee, Wis). The scanning parameters were as follows: detector collimation 4 × 1.25 mm; helical pitch, 0.75; section thickness, 1.25 mm; section interval, 1.25 mm; rotation time, 0.8 s; tube voltage, 120 kVp; tube current, 160–200 mA. To measure the volume of functioning lung, the lung regions with a CT number in the range of −910 to −500 HU were extracted on the workstation, according to the method proposed by Wu et al. [13]. After the lobe to be resected was traced on transaxial CT images within the region of interest (ROI), the functioning lung of CT image after lobectomy was shown on the workstation (AZE Virtual Place, AZE Co. Ltd, Tokyo, Japan) (Fig. 1). Prediction of the PPF by quantitative CT was then conducted according to the following formula:

Predictive postoperative $FEV_1$

= preoperative $FEV_1$

× (1 − target lobe volume/whole lung volume).

### 2.6. SPECT/CT

Lung perfusion scintigraphy images were obtained by SPECT/CT which was composed of a commercially available gantry-free SPECT with dual-head detectors (Skylight; ADAC Laboratories, Milpitas, Calif) and an 8-multidetector-row CT scanner (Light-Speed Ultra Instrument; General Electric, Milwaukee, Wis). The two instruments were juxtaposed so that the CT table carrying the patient could be moved directly into the SPECT scanner before the CT scanning. As a result, each patient was identically positioned for the SPECT and CT imaging.

$^{99m}$Tc-Macroaggregated human serum albumin (MAA: Daiichi Radioisotope Laboratories, Ltd, Tokyo, Japan) was administered intravenously at the dose of 185 MBq, half of the dose administered with the patient in the supine and the remaining half with the patient in the prone position, to allow uniform distribution of the radionuclide.

SPECT data acquisition was performed with a vertex ultra-high resolution parallel-hole (VXUR) collimator. A 360-degree SPECT scan was acquired, and was followed by CT.

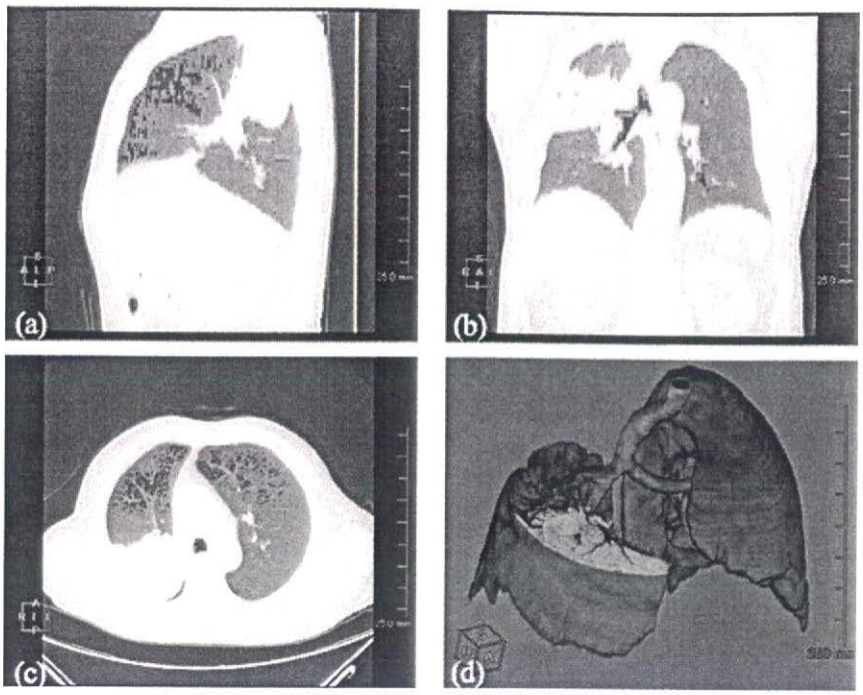


Fig. 1. Quantitative CT in a patient with lung cancer at the hilum of the right upper lobe associated with its peripheral atelectasis. The area with green color shows lung parenchyma with a rage between −910 and −500 HU. The right upper lobe outside of the tumor and atelectasis showed an area without green color due to emphysema. (a) sagittal; (b) coronal; (c) axial; and (d) 3D imaging after virtual lobectomy.

Reconstructive CT images were processed into digital imaging and communications in medicine (DICOM) data and then transferred to a workstation of SPECT/CT (Pegasys: ADAC Laboratories, Milpitas, Calif). One lumen of a three-way stopcock (inner diameter 4 mm, length 10 mm) containing an aqueous solution of $^{99m}Tc\ O_4^-$ and a contrast medium was used as the external fiducial marker. To obtain precise records of both images, the external fiducial markers were fixed to the common platform for the SPECT and CT imaging. The two scans were performed sequentially. Fusion of the SPECT images with the CT images was performed manually by aligning the external fiducial markers of the two images on the workstation. Transaxial, coronal, and sagittal sections of SPECT and CT were manually fused to obtain the best matching images on the workstation (AZE Virtual Place, AZE Co. Ltd, Tokyo, Japan). Preoperative SPECT/CT had been conducted within one month prior to the surgery.

After the lobe to be resected was traced on a CT image within the ROI, the SPECT image after lobectomy was shown on the workstation (Fig. 2). The PPF was predicted according to the following formula:

Predictive postoperative $FEV_1$ = preoperative $FEV_1$ × (1 − RI count of the target lobe/RI count in the *entire lung before surgery*).

### 2.7. Statistical analysis

Correlations between the measured postoperative $FEV_1$ and the predicted value by the SC, quantitative CT and SPECT/CT were assessed by Pearson's correlations and a regression analysis. The difference between the measured postoperative $FEV_1$ and the predicted value was analyzed with the paired $t$-test. To evaluate the effect size of the paired $t$-test, effect size $r$ was calculated using the $t$ value and the degrees of freedom. The differences between the measured and the predicted values were also compared by the paired $t$-test between the SC and quantitative CT, between the SC and SPECT/CT, and the quantitative CT and SPECT/CT. To evaluate the variation of the values, testing of the limits of agreement was performed by Bland–Altman analysis [15]. Values of $p < 0.05$ were accepted as being significant. All values in the text and table represent the mean ± standard deviation (SD).

## 3. Results

The mean postoperative measured $FEV_1$ value was 1.93 l, while the mean predicted $FEV_1$ values were 1.78, 1.86, and 1.89 l using the SC, CT, and SPECT/CT methods, respectively. Significant correlations between the measured and predicted $FEV_1$ values were seen for all three methods (SC; $r = 0.86$, $p < 0.001$, CT; $r = 0.90$, $p < 0.001$, SPECT/CT; $r = 0.86$, $p < 0.001$).

The mean difference between the measured postoperative $FEV_1$ and the predicted value was the largest with the SC method (0.15 ± 0.28 l), followed by the CT method (0.07 ± 0.24 l) and the SPECT/CT method (0.05 ± 0.28 l) (Table 2). With the paired $t$-test, SPECT/CT and CT methods showed no difference between the predicted and measured $FEV_1$ values ($p = 0.33$, 0.07, respectively), but SC showed the significant difference between the predicted and measured

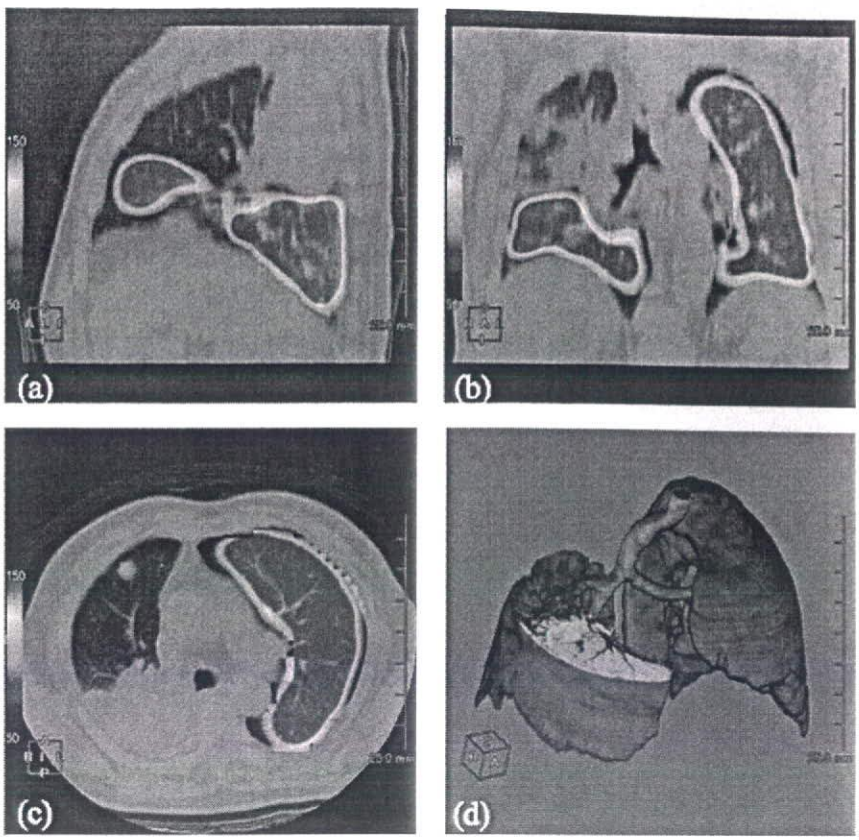


Fig. 2. SPECT/CT of the same slices in Fig. 1. The right upper lobe outside of the tumor and atelectasis showed poor perfusion. (a) sagittal; (b) coronal; (c) axial; and (d) 3D imaging after virtual lobectomy.

$FEV_1$ value ($p < 0.001$). The effect size was the smallest with the SPECT/CT ($r = 0.16$), followed by the quantitative CT ($r = 0.30$) and the SC method ($r = 0.49$).

With the paired $t$-test, the differences between the measured postoperative $FEV_1$ and the predicted value with the SC method were significantly higher than those with the CT method ($p = 0.01$) and the SPECT/CT ($p < 0.001$) (Table 3). However, there was no significant difference of the value between the CT and SPECT/CT ($p = 0.22$).

The range of limits of agreement with the Bland–Altman analysis, i.e., the range of two standard deviations (2 SDs) from the mean difference between the predicted and measured values, was the smallest with the quantitative CT method (from 0.55 to −0.40), followed by the SPECT/CT method (from 0.61 to −0.52) and the SC method (from 0.71 to −0.41) (Fig. 3).

Table 2
Difference between the measured postoperative and the predicted $FEV_1$ in the subsegments counting, quantitative CT, and SPECT/CT methods.

| Method | Difference between the predicted and measured $FEV_1$ (l) | Paired $t$-test | |
|---|---|---|---|
| | | $p$-value | Effect size ($r$) |
| SPECT/CT | 0.05 ± 0.28 | 0.33 | 0.16 |
| CT | 0.07 ± 0.24 | 0.07 | 0.30 |
| SC | 0.15 ± 0.28 | <0.001 | 0.49 |

$FEV_1$: forced expiratory volume in 1 s; SC: subsegments counting; CT: quantitative CT.

Table 3
Comparison of the difference between the measured postoperative and the predicted $FEV_1$ between each method.

| Method | $p$-value with paired $t$-test |
|---|---|
| SC vs CT | 0.01 |
| SC vs SPECT/CT | <0.001 |
| CT vs SPECT/CT | 0.22 |

$FEV_1$: forced expiratory volume in 1 s; SC: subsegments counting; CT: quantitative CT.

## 4. Discussion

The present study confirmed the following two points: (1) the SC method is inferior to both the SPECT/CT and the quantitative CT methods for predicting the PPF after lobectomy; and (2) the SPECT/CT and the quantitative CT methods are almost equally accurate for predicting the PPF. The inaccuracy of the SC method is reasonable, because diseases like COPD or interstitial pneumonia are generally not distributed uniformly in lung tissues. On the other hand, because both the SPECT/CT and the quantitative CT methods assess regional pulmonary function [16–22], these two methods can reasonably predict the PPF more accurately than the SC method, probably even in patients with COPD or interstitial pneumonia. While the range of limits of agreement with the Bland–Altman analysis, i.e. the range of 2 SDs, was smaller in CT method than in SPECT/CT, this analysis just

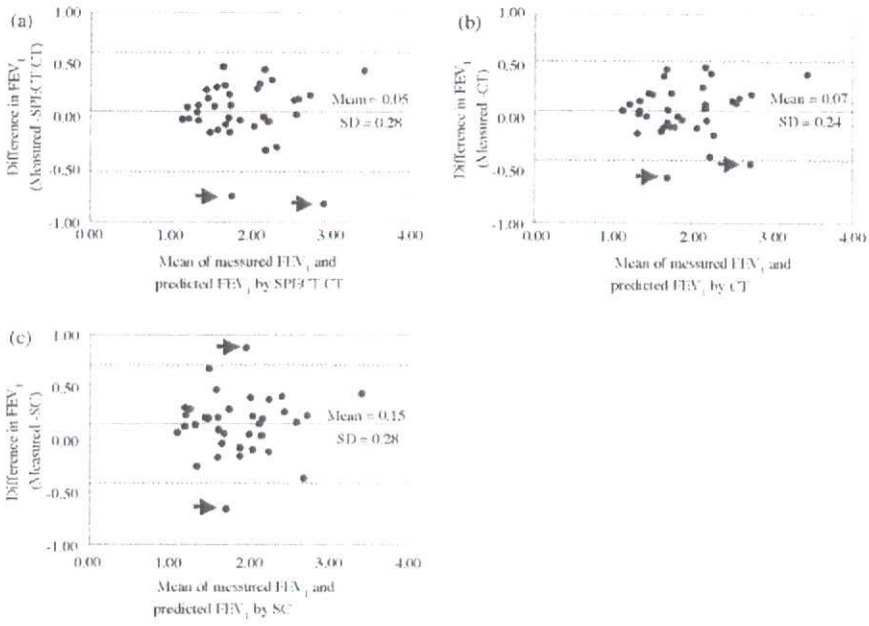


Fig. 3. Bland–Altman analysis. The top and the bottom dotted lines show the range of the limits of agreement between the predicted $FEV_1$ and the measured $FEV_1$ after surgery. (a) SPECT/CT; (b) quantitative CT; (c) subsegments counting method. Arrows show the patients whose predicted $FEV_1$ were out of the range of limits of agreement.

evaluated the variation of the values, which could not rank these methods.

The quantitative CT measurement of lung attenuation has been used to assess the extent of emphysema, and this method has shown a strong correlation with the results of pulmonary function tests [10–12]. Recently, quantitative CT has been applied to the assessment of pulmonary function before lung volume reduction surgery [19–21]. A threshold of −910 HU can exclude emphysema [10,12], while a threshold of −500 HU can exclude areas of air-space loss resulting from tumors or non-tumor-related lesions, such as fibrosis [19,22]. Therefore, the surgical removal of lung areas with a CT number outside of the range of −910 to −500 HU is not expected to cause a loss of lung function. Wu et al. assessed functioning lung tissue with a CT number between −910 and −500 HU and compared the predicted postoperative $FEV_1$ between perfusion scintigraphy and quantitative CT, showing similar correlations for these two methods with the measured postoperative $FEV_1$ [13]. However, their perfusion scintigraphy data was based on planar imaging, which does not enable an accurate delineation of the lobe to be resected. Moreover, 28 of the 44 patients (64%) in their study underwent a pneumonectomy, for which the PPF can be easily predicted, even using planar imaging of scintigraphy. The present study showed that while quantitative CT was superior to SC for predicting the PPF after lobectomy, its accuracy was inferior to that of SPECT/CT.

Recently, Ohno et al. reported that perfusion SPECT/CT allowed a more accurate prediction of the PPF after lobectomy than SPECT [9]. While our results were consistent with those of Ohno et al., our study differed from theirs with respect to the SPECT/CT procedure, as follows: (1) they conducted CT imaging at the end of full inspiration, while we conducted it during the phase of stable expiration to decrease the gap in the images between SPECT and CT; (2) they used commercially available software to fuse the SPECT and CT images, while we fused the two images manually; and (3) they injected the tracer in a single bolus with the patient in a supine position, while we injected half of the dose with the patient in a supine position and the remaining half with the patient in a prone position.

While the present study showed the superiority of both of the CT and SPECT/CT methods to the SC method, there was no significant difference between the former two. The CT method has several advantages over SPECT/CT as the followings: (1) the quantitative CT method is available with the preoperative routine CT examination; (2) less expensive (US $132 vs $431 in Japan); (3) lower radiation exposure; and (4) less time required for the examination (5 min vs 30 min). Therefore, the quantitative CT method could be used in place of the perfusion SPECT/CT method for the prediction of PPF after lung lobectomy.

## References

[1] Zeiher BG, Gross TJ, Kern JA, Lanza LA, Peterson MW. Predicting postoperative pulmonary function in patients undergoing lung resection. Chest 1995;108:68–72.
[2] Ali MK, Mountain CF, Ewer MS, Johnston D, Haynie TP. Predicting loss of pulmonary function after pulmonary resection for bronchogenic carcinoma. Chest 1980;77:337–42.
[3] Cordiner A, De Carlo F, De Gennaro R, Pau F, Flore F. Prediction of postoperative pulmonary function following thoracic surgery for bronchogenic carcinoma. Angiology 1991;42:985–9.
[4] Nakahara K, Monden Y, Ohno K, Miyoshi S, Maeda H, Kawashima Y. A method for predicting postoperative lung function and its relation to postoperative complications in patients with lung cancer. Ann Thorac Surg 1985;39:260–5.
[5] BTS guidelines. Guidelines on the selection of patients with lung cancer for surgery. Thorax 2001;56:89–108.

[6] Beckles MA, Spiro SG, Colice GL, Rudd RM. The physiologic evaluation of patients with lung cancer being considered for resectional surgery. Chest 2003;123(Suppl. 1):105S–14S.
[7] Hirose Y, Imaeda T, Doi H, Kokubo M, Sakai S, Hirose H. Lung perfusion SPECT in predicting postoperative pulmonary function in lung cancer. Ann Nucl Med 1993;7:123–6.
[8] Imaeda T, Kanematsu M, Asada S, Seki M, Matsui E, Doi H, Sakai S, Kokubo M, Hirose H. Prediction of pulmonary function after resection of primary lung cancer. Utility of inhalation-perfusion SPECT imaging. Clin Nucl Med 1995;20:792–9.
[9] Ohno Y, Koyama H, Takenaka D, Nogami M, Kotani Y, Nishimura Y, Yoshimura M, Yoshikawa T, Sugimura K. Coregistered ventilation and perfusion SPECT using krypton-81m and Tc-99m-labeled macroaggregated albumin with multislice CT utility for prediction of postoperative lung function in non-small cell lung cancer patients. Acad Radiol 2007;14:830–8.
[10] Hayhurst MD, MacNee W, Flenley DC, Wright D, McLean A, Lamb D, Wightman AJ, Best J. Diagnosis of pulmonary emphysema by computerised tomography. Lancet 1984;2:320–2.
[11] Gould GA, MacNee W, McLean A, Warren PM, Redpath A, Best JJ, Lamb D, Flenley DC. CT measurements of lung density in life can quantitate distal airspace enlargement—an essential defining feature of human emphysema. Am Rev Respir Dis 1988;137:380–92.
[12] Kinsella M, Muller NL, Abboud RT, Morrison NJ, DyBuncio A. Quantitation of emphysema by computed tomography using a "density mask" program and correlation with pulmonary function tests. Chest 1990;97:315–21.
[13] Wu MT, Pan HB, Chiang AA, Hsu HK, Chang HC, Peng NJ, Lai PH, Liang HL, Yang CF. Prediction of postoperative lung function in patients with lung cancer: comparison of quantitative CT with perfusion scintigraphy. AJR Am J Roentgenol 2002;178:667–72.
[14] American Thoracic Society. Standardization of spirometry—1987 update. Am Rev Respir Dis 1987;136:1285–98.
[15] Bland JM, Altman DG. Statistical methods for assessing agreement between two methods of clinical measurement. Lancet 1986;8(1):307–10.
[16] Suga K, Yasuhiko K, Zaki M, Yamashita T, Seto A, Matsumoto T, Matsunaga N. Assessment of regional lung functional impairment with co-registered respiratory-gated ventilation/perfusion SPET-CT images: initial experiences. Eur J Nucl Med Mol Imaging 2004;31:240–9.
[17] Suga K, Kawakami Y, Zaki M, Yamashita T, Shimizu K, Matsunaga N. Clinical utility of coregistered respiratory-gated (99m)Tc-Technegas/MAA SPECT-CT images in the assessment of regional lung functional impairment in patients with lung cancer. Eur J Nucl Med Mol Imaging 2004;31:1280–90.
[18] Zaki M, Suga K, Kawakami Y, Yamashita T, Shimizu K, Seto A, Matsunaga N. Preferential location of acute pulmonary thromboembolism induced consolidative opacities: assessment with respiratory gated perfusion SPECT-CT fusion images. Nucl Med Commun 2005;26:465–74.
[19] Bae KT, Slone RM, Gierada DS, Yusen RD, Cooper JD. Patients with emphysema: quantitative CT analysis before and after lung volume reduction surgery-work in progress. Radiology 1997;203:705–14.
[20] Gierada DS, Slone RM, Bae KT, Yusen RD, Lefrak SS, Cooper JD. Pulmonary emphysema: comparison of preoperative quantitative CT and physiologic index values with clinical outcome after lung-volume reduction surgery. Radiology 1997;205:235–42.
[21] Thurnheer R, Engel H, Weder W, Stammberger U, Laube I, Russi EW, Bloch KE. Role of lung perfusion scintigraphy in relation to chest computed tomography and pulmonary function in the evaluation of candidates for lung volume reduction surgery. Am J Respir Crit Care Med 1999;159:301–10.
[22] Wu MT, Chang JM, Chiang AA, Lu JY, Hsu HK, Hsu WH, Yang CF. Use of quantitative CT to predict postoperative lung function in patients with lung cancer. Radiology 1994;191:257–62.

# Prospective clinical trial of magnetic-anchor–guided endoscopic submucosal dissection for large early gastric cancer (with videos)

**Takuji Gotoda, MD, Ichiro Oda, MD, Katsunori Tamakawa, PhD, Hirohisa Ueda, PhD, Toshiaki Kobayashi, MD, PhD, Tadao Kakizoe, MD, PhD**

Tokyo, Japan

**Background:** The treatment of early gastric cancer (EGC) by endoscopic submucosal dissection (ESD) has been rapidly gaining popularity in Japan. However, the procedure needs a high quality of skill. To facilitate complicated ESD by using a single working-channel gastroscope ("one-hand surgery method"), the magnetic-anchor-guided ESD (MAG-ESD) controlled by an extracorporeal electromagnet was reported to be successful in a porcine model.

**Objectives:** The purpose of this prospective clinical trial was to evaluate the feasibility of MAG-ESD for large EGC located on the gastric body in human beings.

**Design:** Prospective clinical trial at a single center.

**Setting:** National Cancer Center Hospital, Tokyo, Japan.

**Subjects:** From January 2005 to May 2006, 25 patients with EGC >20 mm in diameter, located in the gastric body, and intestinal-type histology were enrolled. Patients with a cardiac pacemaker, advanced malignancy in other organs, severe cardiac and/or pulmonary diseases, and uncontrolled hypertension and/or diabetes mellitus were excluded from this study.

**Interventions:** Similar to a standard ESD, the MAG-ESD procedure was performed with the patient under conscious sedation by intravenous injection of midazolam (3–5 mg) and pentazocine (15 mg).

**Main Outcome Measurements:** Unfavorable events and other intraoperative complications caused by the magnetic anchor or the magnetic force were recorded and evaluated. Two GI endoscopists (T.G., I.O.) assessed whether the magnetic anchor facilitated gastric ESD according to 2 criteria: "supportive" and "not supportive." The en bloc resection rate, complications, total operation time, bleeding, perforation, and recurrence rate were also evaluated. The total operation time was measured from insertion to withdrawal of the endoscope, including the retrieving of the magnetic anchor or anchors.

**Results:** All tumors were resected en bloc, without any perforations or severe uncontrollable bleeding. All magnetic anchors were safely retrieved. Two endoscopists assessed that the MAG system was supportive in 23 patients. None of the patients experienced physiologic and mental abnormalities as a result of long-term magnetic-field exposure. During a median follow-up of 20 months (15–32 months), neither delayed adverse effects nor allergies caused by the stainless steel of the magnetic anchor were observed.

**Conclusions:** MAG-ESD is a feasible and safe method that allowed an excellent visualization by suitable tissue tension and facilitated gastric ESD in patients with EGC. The system should be miniaturized to make it applicable in daily clinical practice. (Gastrointest Endosc 2009;69:10-5.)

*Abbreviations: EGC, early gastric cancer; ESD, endoscopic submucosal dissection; IT-knife, insulation-tipped diathermic knife; MAG-ESD, magnetic-anchor-guided endoscopic submucosal dissection.*

DISCLOSURE: *The authors report that there are no disclosures relevant to this publication. This study was supported by a grant-in-aid for the Research on Advanced Medical Technology of the Ministry of Health, Labor and Welfare, and a grant-in-aid for the Third Term Comprehensive 10-year Strategy for Cancer Control, of the Ministry of Health, Labor and Welfare, Japan.*


0016-5107/$36.00
doi:10.1016/j.gie.2008.03.1127

It has been reported that endoscopic submucosal dissection (ESD) of early gastric cancer (EGC) improves the rate of successful en bloc resection.[1,2] An ESD by using an insulation-tipped diathermic knife (IT-knife), developed at the National Cancer Center Hospital, was the first of such techniques.[3,4] Other endoscopic devices for ESD have been developed.[5-7] ESD has been rapidly gaining popularity in Japan, primarily because of its ability to remove larger EGC en bloc, thus reducing a local recurrence caused by a piecemeal resection.[8] However, it is still an

investigational technique and requires a high level of skill from the endoscopists.[9-11]

Endoscopic resection should be safe, effective, and applicable to a wide variety of clinical situations. In particular, when EGC is located in the gastric body, an ESD is more complicated, and the rate of a complete resection is lower than in the gastric antrum.[12] The more difficult extension of the wall and the collection of fluid, including blood and/or gastric juice, hinder the performance of the ESD procedure. Optimal extension of the wall and visualization of the lesion is mandatory for a safe and feasible ESD.

To facilitate a complicated standard ESD procedure performed by using a single working-channel gastroscope (one-hand surgery), the magnetic-anchor–guided ESD (MAG-ESD) controlled by an extracorporeal electromagnet, was developed.[13] We reported that MAG-ESD facilitated the ESD procedure in the porcine model. The purpose of this prospective clinical trial was to evaluate the feasibility of MAG-ESD for large EGC in human beings.

**Capsule Summary**

**What is already known on this topic**

- Endoscopic submucosal dissection (ESD) is useful in the en bloc removal of large gastric lesions, thus reducing the risk of a local recurrence caused by piecemeal resection.
- Magnetic-anchor–guided ESD (MAG-ESD), controlled by an extracorporeal electromagnet, facilitates the standard ESD procedure performed by using a single working-channel gastroscope.

**What this study adds to our knowledge**

- In 25 patients with gastric cancer lesions >20 mm in diameter who underwent magnetic-anchor–guided ESD, all tumors were resected en bloc, without any perforations or severe uncontrollable bleeding, and all magnetic anchors were safely retrieved.
- No patient experienced physiologic or mental abnormalities as a result of long-term magnetic field exposure.

## PATIENTS AND METHODS

### Patients

The purpose of this prospective clinical trial was to evaluate the feasibility of MAG-ESD. Twenty-five patients with EGC >20 mm diameter, located in the gastric body, were enrolled. The patients were first seen on an outpatient basis, and the tumor was assessed by a gastroscopy. From January 2005 to May 2006, all patients with EGC >20 mm in diameter, located in the gastric body, and with intestinal-type histology underwent an ESD on an inpatient basis at the National Cancer Center Hospital, Tokyo, Japan. The ethics committee approved the study, and a detailed written informed consent was obtained from each patient. The presented study was conducted according to the Declaration of Helsinki.

The patients with a cardiac pacemaker, advanced malignancy in other organs, severe cardiac and/or pulmonary diseases, uncontrolled hypertension, and/or diabetes mellitus were excluded from this study. Pregnant or lactating women, and those who wished to become pregnant during the study were also excluded. Patients with tumors with recurrent disease, fibrosis, deeper invasion, or diffuse-type histology were excluded.

### Standard ESD

The standard ESD procedure was initially started by using a standard gastroscope with a single working channel (GIF Q260 or Q240; Olympus Optical Co, Ltd, Tokyo, Japan).[14] Marking dots were placed approximately 5 mm outside the margin of the lesions by using a needle-knife (KD-1L-1; Olympus) and forced coagulation current 20 W (IC C200; ERBE, Tübingen, Germany). First, injection of diluted epinephrine (1:100,000) was performed to raise the submucosal layer and to insert the tip of the IT-knife into the submucosal layer. Then, a small initial incision was made by a standard needle-knife by using 80 W, effect 3 Endocut (ICC200; ERBE). Mucosal cutting at the periphery of the marking dots was circumferentially performed with an IT-knife (KD-610L; Olympus) with 80 W Endocut. After additional submucosal injection of diluted epinephrine, the submucosal layer below the lesion was directly dissected by using the same IT-knife. The final aim was to achieve en bloc resection.

All patients were sedated by intravenous injection of midazolam (3–5 mg) and pentazocine (15 mg), and, if necessary, conscious sedation was maintained with an additional injection of midazolam.

### Magnetic anchor and extracorporeal electromagnetic control system

The magnetic anchor (Pentax Co, Tokyo, Japan) consists of 3 parts: a hand-made magnetic weight, made of magnetic stainless steel (SYS420F), microforceps, and a connecting thread. A 1.0 × 1.0 × 1.5-cm weight was designed to facilitate gastric ESD by use of an extracorporeal hands-free electromagnet, whereby magnetic forces allow a suitable counter-traction for submucosal dissection (Fig. 1). The anchor weight used for this procedure was approximately 6 g.

The magnetic control system (Fig. 2) consists of an electromagnet with up-and-down motion; a movable examination table was made by Tamakawa Co (Sendai, Japan) for use in a standard endoscopic room. The magnetic control system consisted of a 0.68 kOe/100A extracorporeal

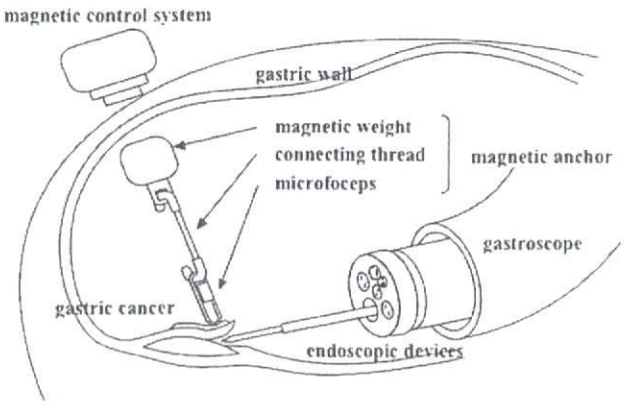


**Figure 1.** Concept of the MAG-ESD.

electromagnet, 350 mm in diameter, positioned at 10 cm from the center of the magnetic yoke. In this manner, the position of the electromagnet was adjusted according to the patient's physique. The examination table was able to move freely to be able to control the magnetic weight so as to achieve ideal mucosal lifting to allow the gastric submucosal dissection.

## MAG-ESD

According to the standard ESD, after circumferential mucosal cutting by using an IT-knife, the procedure was switched to an MAG-ESD, controlled by a high-power electromagnet placed outside the body of the patient (Fig. 3). First, an overtube (Sumitomo Bakelite, Tokyo, Japan) was inserted into the esophagus. Second, a tube catheter was passed through the working channel of the gastroscope. A magnetic anchor, with a magnetic weight, a microforceps, and a connecting thread, was attached to the tip of the catheter. The gastroscope that carries the magnetic anchor was reinserted. Inside the stomach, the magnetic weight was pushed out from the catheter. According to the direction of gravity, the microforceps connected to the magnetic weight was placed at the mucosal edge (Video 1, available online at www.giejournal.org). The submucosal dissection by using an IT-knife was performed by suitable tissue tension with hands-free stabilization and visualization (Video 2, available online at www.giejournal.org).

If experienced endoscopists, who have performed more than 100 gastric ESDs, requested additional magnetic anchors to maneuver the traction direction of the exfoliated gastric tissue, then any numbers of magnetic anchors were attached. To maintain suitable tissue tension, either the patients were rotated or the direction of the magnetic anchor was repositioned by using the movable examination table. After endoscopic resection, both the resected tissue and the magnetic anchor or anchors were retrieved into the overtube by using a grasping forceps and were removed from the stomach.

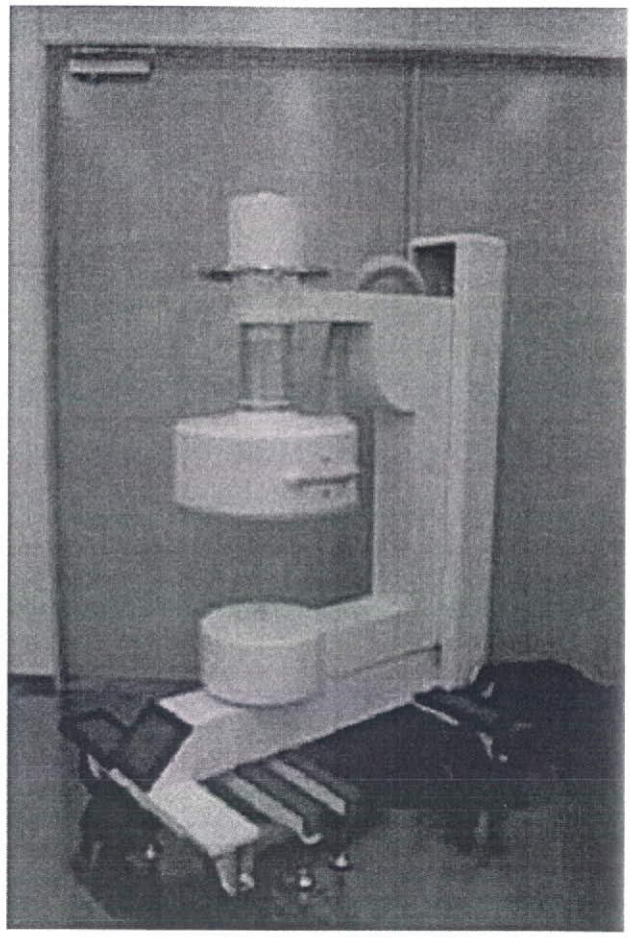

**Figure 2.** Extracorporeal electromagnetic control system.

## Assessments

The demographic and clinical features of each patient were recorded in a case report form. Unfavorable events and other intraoperative complications caused by the magnetic anchor or the magnetic force were recorded and evaluated. We defined serious adverse events as those that lead to death, threat to life, notable disability, prolonged hospital stay, or hospitalization. Patients were followed-up until adverse events either dissipated or returned to pretreatment levels. Two GI endoscopists (T.G., I.O.) assessed, according to the 2 criteria, whether the magnetic anchor facilitated a gastric ESD. Once the dedicated endoscopists evaluated that the MAG-traction–facilitated gastric ESD compared with the standard gastric ESD technique, it was defined as "supportive." When the ESD procedure was not effectively influenced by using the MAG system, it was defined as "not supportive." The en bloc resection rate, complications, total operation time, bleeding, perforation, and recurrence rate were also evaluated. The total operation time was measured from gastroscope insertion to withdrawal, including retrieving the magnetic anchor or anchors.

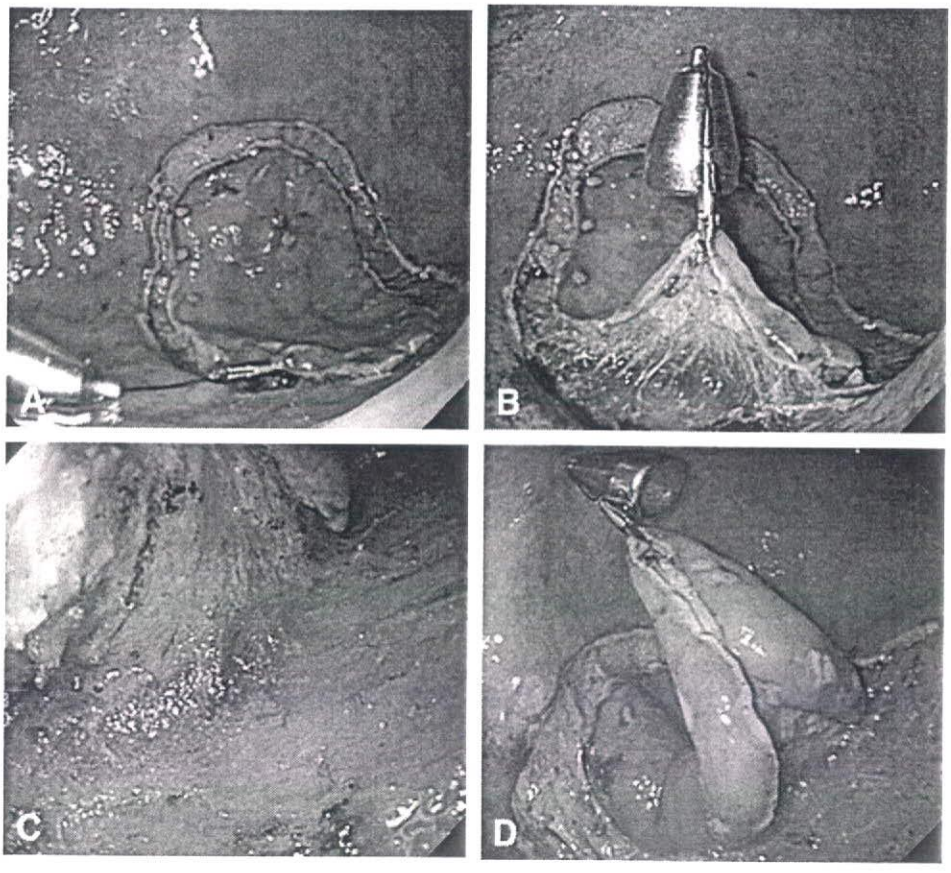


**Figure 3.** Magnetic-anchor–assisted ESD for large EGC. **A,** Fitting the magnetic anchor onto the tip of the gastric mucosa before applying the magnetic force. **B,** Lifting of the gastric tissue and stretched submucosal layer under strong counter-traction by the magnetic anchor. **C,** Good visualization of vessel in submucosal layer under counter-traction by magnetic force. **D,** Controllable traction by the magnetic anchor with a magnetic field.

## RESULTS

The MAG-ESD technique was performed in 25 patients (M/F, 17/8; median age 70 years, range 48-85 years; median tumor size, 30 mm, range 20-70 mm).

The results of the MAG-ESDs are shown in Table 1. All tumors were resected en bloc, without any perforations or severe uncontrollable bleeding. The median size of resected specimen was 55 mm (33-125 mm). The median procedure time was 80 minutes (50-240 minutes). One resection was histologically confirmed as being noncurative because of deep submucosal invasion with positive vertical margins and lymphatic-vessel involvement. This patient underwent additional radical surgery.

One magnetic anchor was required in 21 cases, and 2 magnetic anchors were used in 4 cases. All magnetic anchors were safely retrieved. Two endoscopists assessed that the MAG system was supportive in 23 patients. In particular, the MAG system effectively facilitated an ESD for all 9 tumors located on the greater curvature of the gastric body. However, the magnetic anchor was not helpful in 2 patients. In one case, it was difficult to inflate the gastric lumen because of air leakage through the hiatus hernia.

**TABLE 1. Results of 25 patients treated by MAG-ESD**

| | |
|---|---|
| En bloc resection rate | 25/25 (100%) |
| Median resection size (mm) | 55 (range 33-125) |
| Complications | 0/25 (0%) |
| Median time consumption (min) | 80 (range 50-240) |
| Exposure time for magnetic field (min) | 30 (range 10-110) |
| Endoscopist's assessment | |
| Supportive | 23 |
| Not supportive | 2 |

In another case, it was impossible to pull the gastric tissue toward the proper direction, even after changing the patient's position.

None of the patients experienced physiologic and mental abnormalities as a result of long-term magnetic-field exposure, neither before nor after the procedure. After a mean of 30 minutes (range 10–110 minutes) of exposure

to the magnetic field, no adverse effects of standard ESD procedure were observed regarding pulmonary and cardiac function. During a median follow-up of 20 months (range 15–32 months), neither delayed adverse effects nor allergies were observed because of the stainless steel of the magnetic anchor.

Eight weeks after an MAG-ESD, all artificial defects caused by ESD were completely cured. Neither recurrent cancer nor distant metastases were observed in any of the patients during follow-up.

## DISCUSSION

The present study is, to our knowledge, the first clinical trial by using MAG-ESD for EGC in human beings. The feasibility of the technique for gastric cancer treatment was already evaluated in an animal study. The MAG-ESD technique permits excellent visualization of the submucosal layer, because it is possible to achieve suitable tissue tension. This simplifies a gastric ESD, even for large lesions located in the gastric body. The long-term exposure to the magnetic field did not cause any unwanted physiologic or mental effects. Furthermore, no delayed complications or allergies related to the stainless steel of the magnetic anchor were observed. All the tumors were resected en bloc, without any perforation or severe uncontrollable bleeding.

Endoscopic resection is comparable in many respects to conventional surgery, with the advantages of being less invasive and more cost efficient.[15,16] Endoscopic removal of cancer was initially attempted by using colorectal polypectomy with a high-frequency electric surgical cautery.[17] The use of endoscopic polypectomy to treat pedunculated or semipedunculated EGC was first described in 1974 in Japan. In 1984, the technique of EMR, the so-called strip biopsy, was devised for endoscopic snare polypectomy.[18] Today, EMR is established and widely accepted as a minimally invasive treatment for EGC.[19] Although several techniques have been reported to make EMR procedures easier and safer,[20,21] these cannot be used to remove, en bloc, lesions larger than 2 cm in diameter.[22,23] Piecemeal resection may cause the pathologist to inadequately stage the specimen. Furthermore, there is a high risk of a recurrence after a piecemeal resection.[24,25]

An ESD is superior to a standard EMR and provides en bloc specimens with a standard single-channel gastroscope. After an endoscopic resection, pathologic assessment of depth of cancer invasion, degree of cancer differentiation, and lymphatic or blood-vessel involvement allows an accurate prediction of the risk of lymph-node metastasis.[26] The risk of developing lymph-node or distant metastasis is then weighed against the risk of surgery.[27-29]

Endoscopic resection should be safe, effective, and applicable to a wide variety of clinical situations. However, an ESD still requires an experienced endoscopist with a high level of skill, especially when using a single working-channel gastroscope. Recently, the technique of percutaneous traction-assisted EMR by using a laparoscopic port to create a strong counter-traction was reported.[30-32] However, all previous trials showed that the technique was complicated, invasive, and did not make ESD easier.

Magnets and magnetic fields were used to direct the catheter tip during catheter procedures.[33] A magnetic anchoring system was used to achieve laparoscopic surgery by using a single trocar.[34] Very recently, the feasibility of using magnetically anchored instruments was reported as a promising technique to facilitate natural orifice transluminal endoscopic surgery in a porcine model.[35] These magnets may also provide a way to alter tissue contours without any direct contact. A direct-current–generated magnetic field, as used in magnetic resonance imaging, is regarded as the least invasive or even the most appropriate noninvasive procedure that can be medically applied.

In 21 of our patients, only one magnetic anchor was needed to achieve the desired result, either by rotating the patient or by moving the examination table. In 4 cases, 2 magnetic anchors were required. In 2 cases, a second magnetic anchor was helpful. With the other 2 cases, however, the second anchor did not help, because the MAG system did not provide adequate visualization for submucosal dissection or allow suitable maneuvering of the endoscopic devices. This was caused by underinflation of the gastric cavity. Therefore, to obtain better visualization during an MAG-ESD, the prevention of air leakage because of a hiatus hernia should be achieved.

Another limitation of this procedure was that the extracorporeal electromagnetic control system is too large and cumbersome. Although it was possible to achieve hands-free fixation of the mucosa by using the magnetic anchor tractioned with the extracorporeal electromagnet, the system should be miniaturized to allow wider clinical application.

In conclusion, this prospective clinical trial proved that MAG-ESD can feasibly be used in human beings. The MAG-ESD technique was able to obtain excellent visualization by suitable tissue tension and to facilitate the procedures. Further innovations are warranted to apply the MAG procedure in daily clinical practice.

## ACKNOWLEDGMENTS

We thank Professor Stefan Seewald (Department of Interdisciplinary Endoscopy, University Medical Center Hamburg-Eppendorf, Hamburg, Germany) for his helpful suggestions for fluent medical English and encouragement with the preparation of the article.

## REFERENCES

1. Ono H, Kondo H, Gotoda T, et al. Endoscopic mucosal resection for treatment of early gastric cancer. Gut 2001;48:225-9.

2. Ohkuwa M, Hosokawa K, Boku A, et al. New endoscopic treatment for intramucosal gastric tumors using an insulated-tip diathermic knife. Endoscopy 2001;33:221-6.
3. Hosokawa K, Yoshida S. Recent advances in endoscopic mucosal resection for early gastric cancer [Japanese with English abstract]. Jpn J Cancer Chemother 1998;25:476-83.
4. Gotoda T, Kondo H, Ono H, et al. A new endoscopic mucosal resection (EMR) procedure using an insulation-tipped diathermic (IT) knife for rectal flat lesions. Gastrointest Endosc 1999;50:560-3.
5. Oyama T, Kikuchi Y. Aggressive endoscopic mucosal resection in the upper GI tract: Hook knife EMR method. Minim Invasive Ther Allied Technol 2002;11:291-5.
6. Yahagi N, Fujishiro M, Kakushima N, et al. Endoscopic submucosal dissection for early gastric cancer using the tip of an electrosurgical snare (thin type). Dig Endosc 2004;16:34-8.
7. Yamamoto H, Kawata H, Sunada K, et al. Successful en bloc resection of large superficial tumors in the stomach and colon using sodium hyaluronate and small-caliber-tip transparent hood. Endoscopy 2003; 35:690-4.
8. Oka S, Tanaka S, Kaneko I, et al. Advantage of endoscopic submucosal dissection compared with EMR for early gastric cancer. Gastrointest Endosc 2006;64:877-83.
9. Rösch T, Sarbia M, Schmacher B, et al. Attempted endoscopic en bloc resection of mucosal and submucosal tumors using insulated-tip knives: a pilot series. Endoscopy 2004;36:788-801.
10. Choi IJ, Kim CG, Chang HJ, et al. The learning curve for EMR with circumferential mucosal incision in treating intramucosal gastric cancer. Gastrointest Endosc 2005;62:860-5.
11. Gotoda T, Friedland S, Hamanaka H, et al. A learning curve for advanced endoscopic resection. Gastrointest Endosc 2005;62:866-7.
12. Matsushita M, Hajiro K, Okazaki K, et al. Endoscopic mucosal resection of gastric tumors located in the lesser curvature of the upper third of the stomach. Gastrointest Endosc 1997;45:512-5.
13. Kobayashi T, Gotoda T, Tamakawa K, et al. Magnetic anchor for more effective endoscopic mucosal resection. Jpn J Clin Oncol 2004;34: 118-23.
14. Gotoda T. A large endoscopic resection by endoscopic submucosal dissection (ESD) procedure. Clin Gastroenterol Hepatol 2005;3:S71-3.
15. Soetikno R, Gotoda T, Nakanishi Y, et al. Endoscopic mucosal resection. Gastrointest Endosc 2003;57:567-9.
16. Ludwig K, Klautke G, Bernhard J, et al. Minimally invasive and local treatment for mucosal early gastric cancer. Surg Endosc 2005;19: 1362-6.
17. Deyhle P, Largiader F, Jenny P. A method for endoscopic electroresection of sessile colonic polyps. Endoscopy 1973;5:38-40.
18. Tada M, Murakami A, Karita M, et al. Endoscopic resection of early gastric cancer. Endoscopy 1993;25:445-51.
19. Gotoda T. Endoscopic resection of early gastric cancer: the Japanese perspective. Curr Opin Gastroenterol 2006;22:561-9.
20. Inoue H, Takeshita K, Hori H, et al. Endoscopic mucosal resection with a cap-fitted panendoscope for esophagus, stomach, and colon mucosal lesions. Gastrointest Endosc 1993;39:58-62.
21. Akiyama M, Ota M, Nakajima H, et al. Endoscopic mucosal resection of gastric neoplasms using a ligating device. Gastrointest Endosc 1997;45:182-6.
22. Korenaga D, Haraguchi M, Tsujitani S, et al. Clinicopathological features of mucosal carcinoma of the stomach with lymph node metastasis in eleven patients. Br J Surg 1986;73:431-3.
23. Ell C, May A, Gossner L, et al. Endoscopic mucosectomy of early cancer and high-grade dysplasia in Barrett's esophagus. Gastroenterology 2000;118:670-7.
24. Tanabe S, Koizumi W, Mitomi H, et al. Clinical outcome of endoscopic aspiration mucosectomy for early stage gastric cancer. Gastrointest Endosc 2002;56:708-13.
25. Eguchi T, Gotoda T, Oda I, et al. Is endoscopic one-piece mucosal resection essential for early gastric cancer? Dig Endosc 2003;15:113-6.
26. Gotoda T, Sasako M, Ono H, et al. An evaluation of the necessity of gastrectomy with lymph node dissection for patients with submucosal Invasive gastric cancer. Br J Surg 2001;88:444-9.
27. Gotoda T, Yanagisawa A, Sasako M, et al. Incidence of lymph node metastasis from early gastric cancer: estimation with a large number of cases at two large centers. Gastric Cancer 2000;3:219-25.
28. Etoh T, Katai H, Fukagawa T, et al. Treatment of early gastric cancer in the elderly patient: results of EMR and gastrectomy at a national referral center in Japan. Gastrointest Endosc 2005;62:868-71.
29. Soetikno R, Kaltenbach T, Yeh R, et al. Endoscopic mucosal resection for early cancers of the upper gastrointestinal tract. J Clin Oncol 2005;23:4490-8.
30. Ohashi S. Laparoscopic intraluminal surgery for early gastric cancer: is it a new concept in laparoscopic intraluminal surgery. Surg Endosc 1995;9:169-71.
31. Ohgami M, Otani Y, Kumai K, et al. Curative laparoscopic surgery for early gastric cancer: five years experience. World J Surg 1999;23: 187-93.
32. Kondo H, Gotoda T, Ono H, et al. Percutaneous traction-assisted EMR by using an insulation-tipped electrosurgical knife for early stage gastric cancer. Gastrointest Endosc 2004;59:284-8.
33. Faddis MN, Blume W, Finney J, et al. Novel, magnetically guided catheter for endocardial mapping and radiofrequency catheter ablation. Circulation 2002;106:2980-5.
34. Zeltser IS, Bergs R, Fernandez R, et al. Single trocar laparoscopic nephrectomy using magnetic anchoring and guidance system in the porcine model. J Urol 2007;178:288-91.
35. Scott DJ, Tang SJ, Fernandez R, et al. Completely transvaginal NOTES cholecystectomy using magnetically anchored instruments. Surg Endosc 2007;21:2308-16.

Received December 7, 2007. Accepted March 31, 2008.

Current affiliations: Endoscopy Division (T.G., I.O.), National Cancer Center Hospital, Tokyo, Tamakawa Corporation (K.T.), Sendai, Pentax Corporation (H.U.), Tokyo, Cancer Screening Technology Division (T. Kobayashi), Research Center for Cancer Prevention and Screening, National Cancer Center (T. Kakizoe), Tokyo, Japan.

Reprint requests: Takuji Gotoda, MD, Endoscopy Division, National Cancer Center Hospital, 5-1-1 Tsukiji, Chuo-ku, Tokyo 104-0045, Japan.

If you want to chat with an author of this article, you may contact him at tgotoda@ncc.go.jp.

# Epidermal Growth Factor Receptor Mutations in Multicentric Lung Adenocarcinomas and Atypical Adenomatous Hyperplasias

*Koei Ikeda, MD, PhD,* Hiroaki Nomori, MD, PhD,* Yasuomi Ohba, MD,* Hidekatsu Shibata, MD,* Takeshi Mori, MD, PhD,* Yumi Honda, MD, PhD,† Ken-ichi Iyama, MD, PhD,† and Toshiaki Kobayashi, MD, PhD‡*

**Background:** The mechanisms of generation and progression of multicentric lung adenocarcinoma (AD), bronchioloalveolar carcinoma (BAC), and atypical adenomatous hyperplasia (AAH) in the peripheral lung is not well known. In this study, we analyzed epidermal growth factor receptor (EGFR) mutations in the cases of multicentric AD, BAC, and AAH to reveal the role of EGFR mutation in their generations and progressions.

**Method:** Ninety-seven AAH, BAC, or AD lesions less than 3 cm in size in 26 patients were surgically resected. Of these, EGFR mutations of the nodules with the highest and the second highest grade of histologic malignancy were examined in each patient by using the peptide nucleic acid-locked nucleic acid polymerase chain reaction (PNA-LNA PCR) clamp method.

**Results:** EGFR mutations could be examined in 48 nodules in the 26 patients. The EGFR mutations were found more frequently in lesions with higher histologic malignancy, ie, 9 of 10 ADs (90%), 16 of 28 BACs (57%), and one of 10 AAHs (10%). In 22 patients who could be examined of EGFR mutations for the two lesions in each patient, only two patients (9%) had the same mutation patterns between the two lesions, whereas 15 patients (68%) had the different statuses and the remaining five (23%) had no mutations.

**Conclusion:** Our data demonstrated that EGFR mutations seem to contribute to the acquisition of malignant potential in the AAH-AD sequence and occur independently in each lesion and in the cases of multicentric AD, BAC, and AAH.

(*J Thorac Oncol.* 2008;3: 467–471)

*Department of Thoracic Surgery, Graduate School of Medical Sciences, Kumamoto University, Kumamoto, Japan; †Department of Surgical Pathology, Kumamoto University Hospital, Kumamoto, Japan; and ‡Department of Assistive Diagnostic Technology, National Cancer Center Hospital, Tsukiji, Chuo-ku, Tokyo, Japan.

Disclosure: The authors declare no conflict of interest.

Supported, in part, by Grant-in-Aid from the Ministry of Health, Labor and Welfare of Japan.

Address for correspondence: Hiroaki Nomori, MD, PhD, Department of Thoracic Surgery, Graduate School of Medical Sciences, Kumamoto University, 1-1-1 Honjo, Kumamoto 860-8556, Japan. E-mail: hnomori@qk9.so-net.ne.jp



ISSN: 1556-0864/08/0305-0467

Recent advances in high-resolution computed tomography and the prevalence of CT screening for lung cancer have increased the detection of multiple ground-glass opacity (GGO) nodules,[1–4] which are often atypical adenomatous hyperplasia (AAH), bronchioloalveolar carcinoma (BAC), and adenocarcinoma (AD). However, the mechanisms of generation and progression of these multiple lesions are still unknown.

The concepts of multistep carcinogenesis during which genetic mutations are sequentially accumulated resulting in the development of invasive tumors have been well established in a number of cancers, including colon and breast cancers.[5,6] Although a hypothesis of multistep carcinogenesis has been also proposed for lung AD, ie, AD develops from AAH to invasive AD through BAC,[7] the signals that cause to either transform into invasive AD or to remain AAH or BAC are still unknown.

It has been reported that ADs with BAC features frequently have epidermal growth factor receptor (EGFR) mutations.[8,9] Recently, the possibility of significant role of EGFR mutation in the carcinogenesis of lung AD was also described. Tang et al. showed that EGFR mutation were frequently observed in normal epithelium of patients with EGFR mutant lung AD and described that EGFR mutation could occur in the early step of AD development.[10] Ji et al. showed a close relationship between EGFR mutation and carcinogenesis of lung AD in the experiments on the transgenic mice.[11] From these reports, we speculate that AAH or BAC lesions in patients with multiple AAH, BAC, and AD lesions could already have EGFR mutations. If the EGFR mutations occurred in an early step of AD development, EGFR tyrosine kinase inhibitors (TKIs) could be one of the treatments for patient with multiple AAH, BAC, and AD lesions, because they are frequently effective for AD with EGFR mutations.[12,13]

In this study, to investigate the role of EGFR mutations in generation and progression of multicentric AD, BAC, and AAH lesions, we examined the EGFR mutations in patients with these lesions.

## PATIENTS AND METHODS

### Patients

Between January 1999 and December 2006, 276 patients with AD, BAC, or AAH lesions underwent surgical

resection in Kumamoto University Hospital. Of these, 30 patients had multiple AAH, BAC, and AD lesions, whereas the 246 patients had single lesion. In the 30 patients with multiple lesions, to rule out intrapulmonary metastasis, two patients with moderately or poorly differentiated AD and two patients with lesions more than 3 cm in size were excluded from this study. As a result, 26 patients with multiple AAH, BAC, and AD lesions that showed GGO images on CT were selected for this study. The pathologic diagnoses were made by two different pathologists (Y.H. and K.I.)according to the 1999 World Health Organization histologic classification.[14,15] The multiple lesions in the present case were denied as metastatic ones, according to the criteria of Martini and Melamed.[16] None of the patients received adjuvant chemo- or radiotherapy before surgery.

The study protocol for examining EGFR mutation from the resected lesions was approved by the Ethics Committee of Kumamoto University Hospital in May 2005. Written informed consent was obtained from all patients for investigation of their EGFR mutations of tumors. The tumors with the highest and the second highest grade of histologic malignancy were defined as the first and second tumors, respectively, in each patient. Then, the DNA extracted from the first and the second tumors was investigated for EGFR mutations.

## Detection of EGFR Mutations

We analyzed exons 18, 19, and 21, because most mutations were known to be clustered in these exons.[17] Because most of the examined nodules were less than 2 cm and the amount of extracted DNA was relatively small, the EGFR mutation statuses were analyzed with the use of peptide nucleic acid-locked nucleic acid polymerase chain reaction (PNA-LNA PCR) clamp methods, which was reported to be more sensitive than conventional direct sequencing.[18,19] Surgically resected specimens were fixed with formalin and embedded in paraffin. All sections were cut from paraffin blocks at a thickness of 5 $\mu$m. DNA extraction and analysis of EGFR mutations were performed by Mitsubishi Kagaku Bio-chemical Laboratories Inc (Tokyo, Japan). Tumor cells were visually dissected, and samples were incubated in 200 $\mu$L of lysis buffer (10 mMTris–HCl pH 8.0, 1 mM EDTA, 0.5% SDS) with 40 $\mu$g of glycogen and 2 $\mu$L of proteinase K (20 mg/mL) and incubated at 56°C overnight. DNA was purified by phenol and chloroform extraction and dissolved in 20 $\mu$L TE (10 mM Tris–HCl pH 8.0, 1 mM EDTA). The details of PNA-LNA clamp methods and the design of PCR primers was followed by Nagai et al.[19] Briefly, all PCR reaction solutions (25 $\mu$L) were based on the Basic Mixture containing 25 mmol/L TAPS (pH 9.3), 50 mmol/L KCl, 2 mmol/L $MgCl_2$, 1 mmol/L 2-mercaptoethanol, 200 $\mu$mol/L each of deoxynucleotide triphosphates, and 1.25 units of Takara Ex *Taq*HS (Takara Bio, Shiga, Japan). For conventional PCR, PCR primers (200 nmol/L each) were added to the Basic Mixture. For PNA-LNA PCR clamp, PCR primers (200 nmol/L each), fluorogenic probes (100 nmol/L each), and a PNA clamp primer (5 $\mu$mol/L) were added to the Basic Mixture. The real-time amplification monitoring for both conventional and the PNA-LNA PCR clamp were done using Smart Cycler II (Cepheid, Sunnyvale, CA). PCR cycling was a 30-second hold at 95°C followed by 45 cycles of 95°C for 3 seconds and 62°C (exon 18 and 19) or 56°C (exon 21) for 30 seconds. Nested PCR for the PNA-LNA PCR clamp was done using the same reaction conditions except that the inner primers and 1 $\mu$L of a $1:10^6$ dilution of the first PCR reaction were used.

## Detection of K-ras mutations

We also analyzed the mutation of K-*ras* exon 2 in the same extracted DNA samples. We used the enriched PCR methods to analyze the K-*ras* mutations, which was reported to be able to detect K-*ras* mutation from small amount of DNA samples.[20]

## Statistical Analysis

All values in the text and tables are given as mean ± SD. Category data were compared using the Fisher exact test. The numeric data were analyzed for significance using the two-tailed Student *t* test. Bonferroni test was used to determine significance for comparisons among three parts. Values of $p < 0.05$ were accepted as significant.

# RESULTS

## Clinicopathological Characteristics

Clinicopathological characteristics of the 26 patients with multiple AAH, BAC, and AD lesions are shown in Table 1. There were 6 men and 20 women. Twenty patients (77%) were never smokers. Two patients (8%) had a familial history of lung cancer within the second degree of kinship. The number of resected lesions in each patient was 1 in 3 patients, 2 in 12, 3 in 4, 4 in 2 and more than 5 (up to 27) in 5.

**TABLE 1.** Patient's Characteristics

| | |
|---|---|
| Mean age (yr; range) | 65 (49–79) |
| Sex | |
| Male | 6 |
| Female | 20 |
| Smoking status | |
| Smoker | 6 |
| Never smoker | 20 |
| Number of lesions in CT | |
| 2 | 8 |
| 3 | 4 |
| 4 | 3 |
| ≥5 | 11 |
| Number of resected lesions | |
| 1 | 3 |
| 2 | 12 |
| 3 | 4 |
| 4 | 2 |
| ≥5 | 5 |
| Location | |
| Bilateral | 10 |
| Unilateral | 16 |
| Total | 26 |

CT, computed tomography.

Pathologic diagnoses of the 97 resected nodules were AAH in 34, BAC in 52, and AD in 10. All of the ADs were well differentiated one with BAC or AAH features except for one, which showed a pure papillary pattern. The mean size was $5 \pm 3$ mm in AAH, $9 \pm 8$ mm in BAC, and $16 \pm 8$ mm in AD. There was a significant difference in the mean sizes among the three groups ($p < 0.05$). Of the 26 patients, two patients had multiple AAH lesions. Six patients had multiple BAC lesions. Eight patients had multiple BAC and AAH lesions. Ten patients had AD with BAC or AAH or both. Of the 97 lesions, 54 were resected by lobectomy, 13 by segmentectomy, and 30 by wedge resection. Bilateral lesions were resected in 10 patients, seven of whom underwent simultaneous bilateral resections. Although lymph node dissections or samplings were performed in all patients, none of the patients had lymph node metastasis. All patients are alive without recurrence (mean observation period: 661 days) except for one patient, who died of another disease. In 10 patients, all of lesions could not be resected because of too many lesions, although all of the nonresected nodules have not grown after surgery.

### Mutation Analysis

In 4 of the 26 patients, only one lesion could be examined for EGFR mutations because only one nodule was resected in two patients and the second tumor were too small to extract sufficient amount of DNA in two patients. As a result, EGFR mutations could be examined for 48 nodules in the 26 patients. EGFR mutations were detected in one of the 10 AAHs (10%), 16 of the 28 BACs (57%), and 9 of the 10 ADs (90%) (Table 2). Thirty-eight lesions of AD or BAC harbored EGFR mutations more frequently than 10 AAH lesions ($p = 0.01$). AD harbored EGFR mutations more frequently than BAC with marginal significance ($p = 0.06$). One AD without EGFR mutation showed a pure papillary pattern without BAC features (Case 8 in Table 3). One AAH with EGFR mutation was histologically high grade one (Case 17 in Table 3).

Of the 48 lesions, 26 (54%) harbored EGFR mutations. The type of mutations in these 26 lesions was exon 21 L858R in 15 lesions (58%), exon 19 deletions in 10 (38%), and exon 21 L861Q in one (4%). Tables 3 and 4 show the mutation statuses of the lesions of the 22 patients who could be examined for the presence of EGFR mutations in both first and second tumors, two patients (9%) showed the same pattern of mutations in each lesion. Fifteen patients (68%) showed different mutational statuses of mutations among the lesions, of whom five patients showed different patterns of mutations between the two lesions and 10 patients had EGFR mutations in only one of the two lesions. Five patients (23%) showed no mutation in both lesions.

K-*ras* mutations were detected in one AAH (10%) and one BAC (4%). Both of them were transversion that changes G to T at codon 12. These K-*ras* mutations were not overlapped with the EGFR mutations.

**TABLE 2.** EGFR Mutations in Each Histological Type

| Histological Type | Number of Nodules (%) | | Total |
|---|---|---|---|
| | With Mutations | Without Mutations | |
| AAH | 1 (10%) | 9 (90%) | 10 |
| BAC | 16 (57%) | 12 (43%) | 28 |
| AD | 9 (90%) | 1 (10%) | 10 |
| Total | 26 (54%) | 22 (46%) | 48 |

EGFR, epidermal growth factor receptor; AAH, atypical adenomatous hyperplasia; BAC, bronchioloalveolar carcinoma; AD, adenocarcinoma.

## DISCUSSION

It has been reported that ADs with BAC features harbor EGFR mutations frequently, ie, 9 of 18 (50%) by Blons et al.,[8] and 14 of 21 (66%) by Hsieh et al.[9] The significant high rate of EGFR mutation was also reported in ADs of East Asian patients (270 of 563, 48%), females (203 of 411, 49%), and nonsmokers (232 of 433, 54%).[21] Although the mutation rate of ADs in our study was 90% (9 of 10), which was higher than those in previous reports, it could be because of the following reasons: (1) All of the patients were East Asian; (2) Twenty of the 26 patients (77%) were female; (3) Twenty of the 26 patients (77%) were nonsmokers; and (4) Nine of the 10 ADs (90%) were well differentiated AD with BAC features.

Our result showed that the EGFR mutation patterns of the first and second tumors were same in only 2 of the 22 patients (9%) and the mutation statuses were different in 15 of the 22 patients (68%). This result demonstrated that EGFR mutations would be independently acquired after multicentric generation of the AAH, BAC, and AD lesions.

A hypothesis of multistep carcinogenesis has been proposed for lung AD, which develops from AAH to invasive AD through BAC.[7] We expected that EGFR mutations might occur in an early step of the AAH-AD sequence, and therefore that the mutation might frequently be detected already in AAH or BAC in patients with multiple AAH, BAC, and AD lesions. However, our results showed that most AAHs did not have EGFR mutations and that BACs had the mutations less frequently than ADs. This result corresponded to that of Yoshida et al., who examined EGFR mutations mostly in solitary AAH, BAC, and AD lesions.[22] We therefore consider that the EGFR mutations would not cause the occurrence of multiple AAH, BAC, and AD lesions and would be acquired independently after multicentric generation of the lesions, and contribute to acquirement of malignant potentials during AAH-AD sequence.

The K-*ras* mutation in AAH was reported to be shown in 8 of 30 lesions (27%) by Yoshida et al.[22] and 13 of 40 (32%) by Sakamoto et al.,[23] of which frequency was higher than the one of 10 (10%) in our study. Although the reason of relatively low frequency of K-*ras* mutation in our study is not clear, it might be a character of our study with multiple neoplastic lesions.

In 10 of the 26 patients, all of the lesions could not be resected because of too many lesions. Because EGFR-TKIs would be effective for AD lesions with EGFR mutations,[12,13,24] we first expected that EGFR-TKIs could be effective for not only AD but also BAC or AAH in these patients. However, our results showed that the EGFR muta-

**TABLE 3.** Patterns of EGFR Mutations in Each Patient

| Case | Age (yr) | Sex | First Tumor | | Second Tumor | |
|---|---|---|---|---|---|---|
| | | | Histological Type | EGFR Mutation | Histological Type | EGFR Mutation |
| 1 | 69 | F | AD | exon19 delE746_A750 | BAC | exon21 L858R |
| 2 | 64 | F | AD | exon21 L858R | BAC | exon21 L858R |
| 3 | 72 | F | AD | exon21 L858R | BAC | None |
| 4 | 55 | M | AD | exon21 L858R | BAC | None |
| 5 | 53 | F | AD | exon19 delL747_S752 | BAC | None |
| 6 | 71 | F | AD | exon19 delL747_S752 | BAC | None |
| 7 | 49 | F | AD | exon21 L858R | BAC | exon19 delE746_A750 |
| 8 | 79 | F | AD | None | BAC | exon21 L858R |
| 9 | 61 | F | AD | exon19 delL747_S752 | AAH | None |
| 10 | 66 | F | AD | exon21 L858R | AAH | None |
| 11 | 63 | F | BAC | exon19 delE746_A750 | BAC | exon21 L858R |
| 12 | 76 | F | BAC | exon21 L858R | BAC | exon21 L858R |
| 13 | 72 | M | BAC | exon21 L861Q | BAC | exon21 L858R |
| 14 | 65 | F | BAC | exon21 L858R | BAC | None |
| 15 | 79 | F | BAC | exon21 L858R | BAC | None |
| 16 | 54 | F | BAC | None | BAC | None |
| 17 | 73 | M | BAC | exon19 delS752_I758 | AAH | exon19 L747_T751 |
| 18 | 74 | F | BAC | exon19 delE746_A750 | AAH | None |
| 19 | 57 | M | BAC | None | AAH | None |
| 20 | 47 | F | BAC | None | AAH | None |
| 21 | 58 | F | BAC | None | AAH | None |
| 22 | 57 | M | AAH | None | AAH | None |

EGFR, epidermal growth factor receptor; M, male; F, female; AAH, atypical adenomatous hyperplasia; BAC, bronchioloalveolar carcinoma; AD, adenocarcinoma; NE, not examined.

**TABLE 4.** Pattern of EGFR Mutations of the Two Lesions in Each Patient

| | |
|---|---|
| Same mutation pattern | 2 (9%) |
| Different mutation patterns | 5 (23%) |
| Mutation in one of the two lesions | 10 (45%) |
| No mutation in both lesions | 5 (23%) |
| Total | 22 |

EGFR, epidermal growth factor receptor.

tions were rare in AAH and were less frequent in BAC than in AD. Therefore, EGFR-TKIs might not be effective for AAH and BAC in the patients with multiple AAH, BAC, and AD lesions.

Although CT guided needle aspiration biopsy is a minimally invasive method for histologic diagnosis, it has some difficulties to differentiate boundary lesions. Our study showed that 90% of ADs in multiple GGO nodules had EGFR mutations, whereas 90% of AAHs did not. Because PNA-LNA PCR clamp method can detect EGFR mutations of small tumor tissues with higher sensitivity than the conventional direct sequencing,[18,19] we believe that the EGFR mutation analysis in the specimens obtained by needle biopsy would contribute to a pathologic diagnosis and prediction of malignant grade of GGO nodules. For example, when the EGFR mutations were positive in biopsy specimens of GGO nodules, which were suspected of AAH or BAC with histologic findings, surgical resection could be recommended because of high possibility of high grade of BAC. When EGFR mutations were negative for GGO nodules, which were suspected of AAH or BAC with histologic findings, follow-up could be one of the choices because of high possibility of AAH or low grade of BAC.

In conclusion, EGFR mutations independently occurred after mulicentric generation of lung cancers. In addition, there was close relationship between the histologic malignancy grade and EGFR mutations in patients with multiple AAH, BAC, and AD lesions. Although EGFR mutations would not to be involved in generation of multiple AAH, BAC, and AD lesions, they seem to contribute to the acquisition of malignant potential in the AAH-AD sequence. We believe that our results would contribute to a guideline of clinical management of patients with multiple GGO nodules.

## REFERENCES

1. Nomori H, Ohtsuka T, Naruke T, et al. Histogram analysis of computed tomography numbers of clinical T1 N0 M0 lung adenocarcinoma, with special reference to lymph node metastasis and tumor invasiveness. *J Thorac Cardiovasc Surg* 2003;126:1584–1589.
2. Kodama K, Higashiyama M, Yokouchi H, et al. Prognostic value of ground-glass opacity found in small lung adenocarcinoma on high-resolution CT scanning. *Lung Cancer* 2001;33:17–25.
3. Aoki T, Nakata H, Watanabe H, et al. Evolution of peripheral lung adenocarcinomas: CT findings correlated with histology and tumor doubling time. *AJR Am J Roentgenol* 2000;174:763–768.
4. Mirtcheva RM, Vazquez M, Yankelevitz DF, et al. Bronchioloalveolar

carcinoma and adenocarcinoma with bronchioloalveolar features presenting as ground-glass opacities on CT. *Clin Imaging* 2002;26:95–100.
5. Vogelstein B, Fearon ER, Hamilton SR, et al. Genetic alterations during colorectal-tumor development. *N Engl J Med* 1988;319:525–532.
6. Beckmann MW, Niederacher D, Schnürch HG, et al. Multistep carcinogenesis of breast cancer and tumour heterogeneity. *J Mol Med* 1997;75: 429–439.
7. Kitamura H, Kameda Y, Ito T, et al. Atypical adenomatous hyperplasia of the lung. Implications for the pathogenesis of peripheral lung adenocarcinoma. *Am J Clin Pathol* 1999;111:610–622.
8. Blons H, Côté JF, Le Corre D, et al. Epidermal growth factor receptor mutation in lung cancer are linked to bronchioloalveolar differentiation. *Am J Surg Pathol* 2006;30:1309–1315.
9. Hsieh RK, Lim KH, Kuo HT, et al. Female sex and bronchioloalveolar pathologic subtype predict EGFR mutations in non-small cell lung cancer. *Chest* 2005;128:317–321.
10. Tang X, Shigematsu H, Bekele BN, et al. EGFR tyrosine kinase domain mutations are detected in histologically normal respiratory epithelium in lung cancer patients. *Cancer Res* 2005;65:7568–7572.
11. Ji H, Li D, Chen L, et al. The impact of human EGFR kinase domain mutations on lung tumorigenesis and in vivo sensitivity to EGFR-targeted therapies. *Cancer Cell* 2006;9:485–495.
12. Jänne PA, Johnson BE. Effect of epidermal growth factor receptor tyrosine kinase domain mutations on the outcome of patients with non-small cell lung cancer treated with epidermal growth factor receptor tyrosine kinase inhibitors. *Clin Cancer Res* 2006;12:4416s–4420s.
13. Riely GJ, Politi KA, Miller VA, et al. Update on epidermal growth factor receptor mutations in non-small cell lung cancer. *Clin Cancer Res* 2006;12:7232–7241.
14. Brambilla E, Travis WD, Colby TV, et al. The new World Health Organization classification of lung tumours. *Eur Respir J* 2001;18: 1059–1068.
15. Travis M, Colvy T, Corrin B, et al. World Health Organization international histological classification of tumors. Histological typing of lung and pleural tumors. 3rd ed. In collaboration with Sobin LH and pathologists from 14 countries. Berlin: Springer-SpVerlag, 1999.
16. Martini N, Melamed MR. Multiple primary lung cancers. *J Thorac Cardiovasc Surg* 1975;70:606–612.
17. Fukuoka M, Yano S, Giaccone G, et al. Multi-institutional randomized phase II trial of gefitinib for previously treated patients with advanced non-small-cell lung cancer (The IDEAL 1 Trial) [corrected]. *J Clin Oncol* 2003;21:2237–2246.
18. Tanaka T, Nagai Y, Miyazawa H, et al. Reliability of the peptide nucleic acid-locked nucleic acid polymerase chain reaction clamp-based test for epidermal growth factor receptor mutations integrated into the clinical practice for non-small cell lung cancers. *Cancer Sci* 2007;98:246–252.
19. Nagai Y, Miyazawa H, Huqun, et al. Genetic heterogeneity of the epidermal growth factor receptor in non-small cell lung cancer cell lines revealed by a rapid and sensitive detection system, the peptide nucleic acid-locked nucleic acid PCR clamp. *Cancer Res* 2005;65:7276–7282.
20. Kubicka S, Kuhnel F, Flemming P, et al. K-ras mutations in the bile of patients with primary sclerosing cholangitis. *Gut* 2001;48:403–408.
21. Shigematsu H, Gazdar AF. Somatic mutations of epidermal growth factor receptor signaling pathway in lung cancers. *Int J Cancer* 2006; 118:257–262.
22. Yoshida Y, Shibata T, Kokubu A, et al. Mutations of the epidermal growth factor receptor gene in atypical adenomatous hyperplasia and bronchioloalveolar carcinoma of the lung. *Lung Cancer* 2005;50:1–8.
23. Sakamoto H, Shimizu J, Horio Y, et al. Disproportionate representation of KRAS gene mutation in atypical adenomatous hyperplasia, but even distribution of EGFR gene mutation from preinvasive to invasive adenocarcinomas. *J Pathol* 2007;212:287–294.
24. Pao W, Miller VA. Epidermal growth factor receptor mutations, small-molecule kinase inhibitors, and non-small-cell lung cancer: current knowledge and future directions. *J Clin Oncol* 2005;23:2556–2568.

 